arXiv:nucl-th/0206070v1 28 Jun 2002

On the analytic solution of the pairing problem: one pair in many levels

M. Barbaro[1], R. Cenni[2], A. Molinari[1] and M. R. Quaglia[2]
[1] Dipartimento di Fisica Teorica — Università di Torino
Istituto Nazionale di Fisica Nucleare — Sez. di Torino
Torino —Italy
[2] Dipartimento di Fisica — Università di Genova
Istituto Nazionale di Fisica Nucleare — Sez. di Genova
Genova — Italy

Abstract

We search for approximate, but analytic solutions of the pairing problem for one pair of nucleons in many levels of a potential well. For the collective energy a general formula, independent of the details of the single particle spectrum, is given in both the strong and weak coupling regimes. Next the displacements of the solutions trapped in between the single particle levels with respect to the unperturbed energies are explored: their dependence upon a suitably defined quantum number is found to undergo a transition between two different regimes.

PACS: 24.10.Cn; 21.60.-n
Keywords: Pairing interaction

1 Introduction

In this paper we deal with the problem of the pairing Hamiltonian for one pair of nucleons living in a set of levels of a potential well.

There are several motivations for this study. First, to find approximate, but analytic, solutions for the eigenvalues and the eigenfunctions, which we believe to be not only interesting *per se*, but also useful for paving the way to the general problem of n interacting pairs (see ref. [1]). Second, to connect the energy of the collective mode, both in the strong and in the weak coupling regime, to global features of the single particle levels spectrum like the variance, the skewness, the kurtosis, etc. Third, to unravel the remarkable pattern displayed by the solutions trapped in between the single particle levels, already hinted at in ref. [2]. Indeed by connecting the trapped solutions to a quantum number λ, it is found that their behaviour versus λ is not only smooth, but displays a transition between two different regimes. Interestingly, this transition may be on one side related to a sort of sum rule obeyed by the trapped eigenvalues (stemming from the Viète conditions for the solutions of an algebraic equation) and on the other to the basic nature of the pairing interaction.

The paper is organised as follows: in section 2 the general formalism is presented and the basic equations are deduced in the framework of the Grassmann variables; in section 3 the collective solution is addressed in both the strong and weak coupling regimes; in section 4 the trapped solutions and their regularities are studied within the harmonic oscillator and related models for the single particle potential well.

2 General formalism

Consider a shell of an average potential well, whose shape needs not to be specified, with L non-degenerate single particle levels of energy e_ν and angular momentum j_ν, the associated multiplicity being $2\Omega_\nu = 2j_\nu + 1$ $(1 \leq \nu \leq L)$.

Let identical fermions (e.g., neutrons) living in this set of levels interact through the pairing force. The Hamiltonian of the system $\hat{H} = \hat{H}_0 + \hat{H}_P$ splits then into a single particle

$$\hat{H}_0 = \sum_{\nu=1}^{L} e_\nu \sum_{m_\nu=-j_\nu}^{j_\nu} \hat{a}^\dagger_{j_\nu m_\nu} \hat{a}_{j_\nu m_\nu} \tag{1}$$

and into a pairing interaction

$$\hat{H}_P = -G \sum_{\mu,\nu=1}^{L} \hat{A}^\dagger_\mu \hat{A}_\nu \tag{2}$$

term. In (2)

$$\hat{A}_\mu = \sum_{m_\mu=1/2}^{j_\mu} (-1)^{j_\mu - m_\mu} \hat{a}_{j_\mu,-m_\mu} \hat{a}_{j_\mu m_\mu} \ , \tag{3}$$

$\hat{a}_{jm}$, $\hat{a}^\dagger_{jm}$ being the nucleon's destruction and creation operators. The operators $\hat{A}_\mu$ and $\hat{A}^\dagger_\mu$ destroy and create pairs having total angular momentum $J = 0$ in the level j_μ.

As well-known, the problem of the Hamiltonian (1,2) has been addressed [1] by first diagonalising the associated bosonic Hamiltonian and then by accounting for the Pauli principle. Here we search for compact, possibly accurate, expressions for the eigenvalues and eigenvectors of $\hat{H}$ and to unravel hidden correlations among the solutions.

We start by recasting the eigenvalue equation in the Bargmann-Fock representation of the hamiltonian formalism, where the odd (anti-commuting) Grassmann variables λ_{jm}, λ^*_{jm} replace the fermionic operators $\hat{a}_{jm}$, $\hat{a}^\dagger_{jm}$. For this purpose we introduce the even variables

$$\varphi_{jm} \equiv (-1)^{j-m} \lambda_{j-m} \lambda_{jm} \ , \tag{4}$$

in terms of which the operators $\hat{A}_\mu$ become

$$\hat{A}_\mu \longrightarrow \Phi_\mu = \sum_{m_\mu=1/2}^{j_\mu} \varphi_{j_\mu m_\mu} \tag{5}$$

and the Hamiltonian (better, the normal kernel of)

$$H = \sum_{\nu=1}^{L} e_\nu \sum_{m_\nu=-j_\nu}^{j_\nu} \lambda^*_{j_\nu m_\nu} \lambda_{j_\nu m_\nu} - G \sum_{\mu,\nu=1}^{L} \Phi^*_\mu \Phi_\nu \ . \tag{6}$$

The index of nil-potency of the collective Grassmann variable Φ_μ (to be referred to as s-quasi-boson) is Ω_μ, i.e.,

$$(\Phi_\mu)^n = 0 \quad \text{for } n > \Omega_\mu \ . \tag{7}$$

We now search for eigenstates of n pairs of fermions in the s-quasibosons subspace as products of n factors, namely

$$\psi_n(\Phi^*) = \prod_{k=1}^{n} \mathcal{B}_k^* \tag{8}$$

where

$$\mathcal{B}_k^* = \sum_{\nu=1}^{L} \beta_\nu^{(k)} \Phi_\nu^* \ , \tag{9}$$

is a superposition of s-quasibosons placed in all the available levels.

For this scope it is convenient to start from the effective Hamiltonian

$$\mathcal{H}_{\rm eff}(\varphi^*, \varphi) = \sum_{\nu=1}^{L} 2e_\nu \sum_{m_\nu=1/2}^{j_\nu} \varphi_{j_\nu m_\nu}^* \varphi_{j_\nu m_\nu} - G \sum_{\mu,\nu=1}^{L} \Phi_\mu^* \Phi_\nu \ , \tag{10}$$

coincident with (6) in the s-quasibosons subspace spanned by the states (8). Indeed while terms like $\lambda^*\lambda$ count the number of particles, $\varphi^*\varphi \equiv \lambda^*\lambda^*\lambda\lambda$ counts the number of pairs. The eigenvalue equation then reads

$$\begin{aligned} H\psi_n(\Phi^*) = \int \left[d\lambda' d\lambda^{*\prime}\right] \mathcal{H}_{\rm eff}(\varphi^*, \varphi') \exp\left(\sum_{\mu=1}^{L} \sum_{m_\mu=-j_\mu}^{j_\mu} \lambda_{j_\mu m_\mu}^* \lambda'_{j_\mu m_\mu}\right) \\ \times \exp\left(-\sum_{\mu=1}^{L} \sum_{m_\mu=-j_\mu}^{j_\mu} \lambda^{*\prime}{}_{j_\mu m_\mu} \lambda'_{j_\mu m_\mu}\right) \psi_n(\Phi^{*\prime}) = E_n \psi_n(\Phi^*) \ , \end{aligned} \tag{11}$$

where

$$[d\lambda^{*\prime} d\lambda'] \equiv \prod_{\nu=1}^{L} \prod_{m_\nu=-j_\nu}^{j_\nu} d\lambda^{*\prime}{}_{j_\nu, m_\nu} d\lambda'_{j_\nu, m_\nu} \ . \tag{12}$$

By expanding the exponentials in (11), only the even powers, hence only the φ variables, survive. Thus (11) can be rewritten as

$$\int [d\varphi^{*\prime} d\varphi'] \mathcal{H}_{\rm eff}(\varphi^*, \varphi') \mathcal{M}(\varphi^* + \varphi^{*\prime}, \varphi') \psi_n(\Phi^{*\prime}) = E_n \psi_n(\Phi^*) \ , \tag{13}$$

where

$$\mathcal{M}(\varphi^*,\varphi) \equiv \exp\left(\sum_{\mu=1}^{L}\sum_{m_\mu=1/2}^{j_\mu} \varphi^*_{j_\mu m_\mu}\varphi_{j_\mu m_\mu}\right) \ . \tag{14}$$

The integrals over the φ's, relevant for dealing with eq. (11), are listed in [3, 4]. One gets

$$E_n = \sum_{k=1}^{n}\eta_k \ , \qquad \beta_\mu^{(k)} = \frac{1}{2e_\mu - \eta_k} \ , \tag{15}$$

the η_k being the solutions of the non-linear system

$$\sum_{\mu=1}^{L}\frac{\Omega_\mu}{2e_\mu-\eta_k} - \sum_{\substack{l=1\\ l\neq k}}^{n}\frac{1}{\eta_l-\eta_k} = \frac{1}{G} \ . \tag{16}$$

In this paper we confine ourselves to the case of a single pair only. Then (16) reduces to a single equation and the wave function reads

$$\psi_1(\Phi^*) = \sum_{\nu=1}^{L}\beta_\nu\Phi^*_\nu \ . \tag{17}$$

Since the action of H on (17) is

$$\begin{aligned} &H\psi_1(\Phi^*) \\ &\quad= \sum_{\nu=1}^{L}2e_\nu\sum_{\mu=1}^{L}\beta_\mu\sum_{m_\nu=1/2}^{j_\nu}\varphi^*_{j_\nu m_\nu}\int[d\varphi^{*\prime}d\varphi']\varphi'_{j_\nu m_\nu}\mathcal{M}(\varphi^*+\varphi^{*\prime},\varphi')\Phi^{*\prime}_\mu \\ &\quad -G\sum_{\mu,\nu=1}^{L}\sum_{\rho=1}^{L}\beta_\rho\Phi^*_\mu\int[d\varphi^{*\prime}d\varphi']\Phi'_\nu\mathcal{M}(\varphi^*+\varphi^{*\prime},\varphi')\Phi^{*\prime}_\rho \\ &\quad= \sum_{\nu=1}^{L}2e_\nu\beta_\nu\Phi^*_\nu - G\sum_{\mu,\nu=1}^{L}\Omega_\mu\beta_\mu\Phi^*_\nu \ , \end{aligned} \tag{18}$$

the Schrödinger equation becomes

$$\sum_{\nu=1}^{L}\left[(2e_\nu - E)\beta_\nu - G\sum_{\mu=1}^{L}\Omega_\mu\beta_\mu\right]\Phi^*_\nu = 0 \tag{19}$$

which implies

$$(2e_\nu - E)\beta_\nu - G\sum_{\mu=1}^{L}\Omega_\mu\beta_\mu = 0 \qquad \forall\nu = 1, L \ . \tag{20}$$

Since $\sum_{\mu=1}^{L}\Omega_\mu\beta_\mu$ does not depend on the index ν, it follows that the coefficients β_ν are

$$\beta_\nu = \frac{C}{2e_\nu - E} \ , \tag{21}$$

C being a normalisation factor. Inserting (21) into (20) we then get the well-known eigenvalue equation (referred to in the following as secular equation) [5]

$$\sum_{\nu=1}^{L}\frac{\Omega_\nu}{2e_\nu - E} = \frac{1}{G} \ , \tag{22}$$

which yields L eigenvalues $E^{(\mu)}$ $(1 \leq \mu \leq L)$, the corresponding components $\beta_\nu^{(\mu)}$ of the wave function being given by eq. (21).

Actually the normalisation of the state

$$(\psi_1^*, \psi_1) = \sum_{\nu,\nu'=1}^{L}\beta_\nu^*\beta_{\nu'}\,(\Phi_\nu, \Phi_{\nu'}^*) = \sum_{\nu=1}^{L}\Omega_\nu|\beta_\nu|^2 = 1 \tag{23}$$

suggests to introduce the coefficients

$$\tilde{\beta}_\nu^{(\mu)} = \sqrt{\Omega_\nu}\beta_\nu^{(\mu)} \ . \tag{24}$$

It is straightforward to solve equation (22) numerically: the solutions can be graphically displayed as the intersections of the lhs of (22) with the straight line $E = 1/G$. In Fig. 1 this is done for 5 levels of a 3-dimensional harmonic oscillator and for two typical values of $\tilde{G} \equiv G/\hbar\omega_0$. In the figure two classes of states (labelled as $k = 0, \ldots, \mathcal{N} - 1$) appear: the first one embodying the $k = 0$ state, which lies below the lowest single particle level for an attractive interaction and corresponds to a collective state; the other embodies the so-called "trapped" solutions $(1 \leq k \leq 4)$, which lie in between the single particle levels.

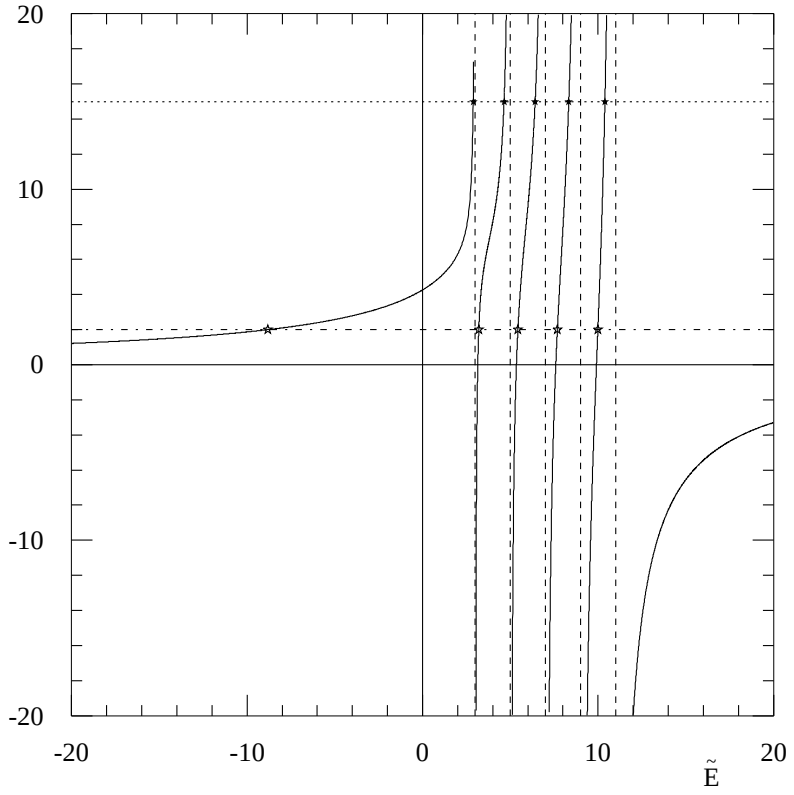

Figure 1: Graphical solution of the eq. (22) for the case of a harmonic oscillator well with 5 levels. The values of $\tilde{G}$ are 1/2 (dot-dashed) and 1/15 (dotted). All quantities are in dimensionless units ($\tilde{E} = E/\hbar\omega_0$).

The collective and single particle character of the eigenstates is apparent in the histograms of Fig. 2, where the coefficients $\tilde{\beta}_h^{(k)}$ are displayed. The states on the left panel correspond to the coupling constant $\tilde{G} = 1/2$, those on the right panel to $\tilde{G} = 1/15$. From the top to the bottom the coefficients of the collective ($k = 0$) and of the trapped ($1 \leq k \leq 4$) states are shown. The bars, from left to right, yield the components $h = 0, \cdots 4$ of the wave

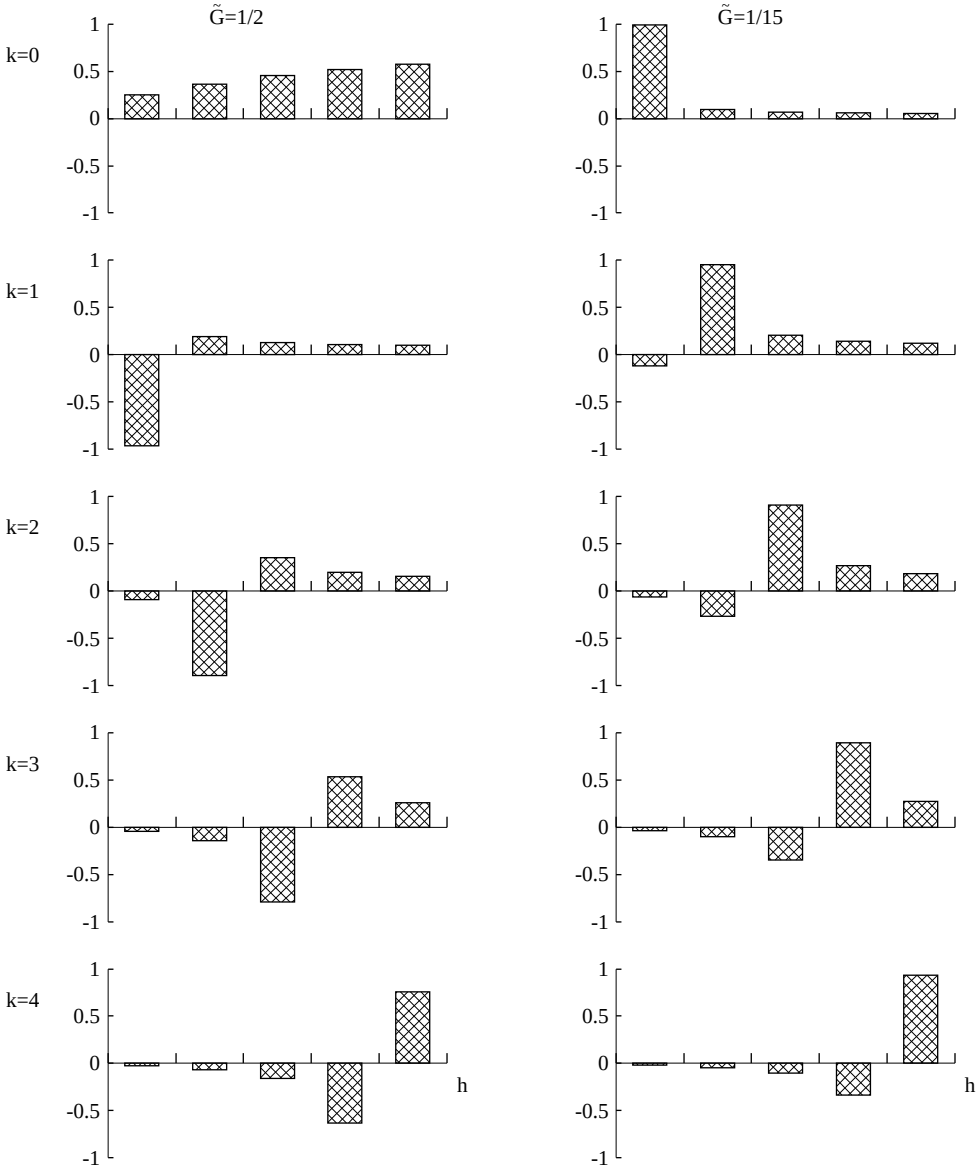

Figure 2: The wave functions components, $\tilde{\beta}_h^{(k)}$, of the collective and trapped states (from top to bottom) for $\tilde{G} = 1/2$ (left panel) and $\tilde{G} = 1/15$ (right panel) in the same case as in Fig. 1.

functions

$$\psi_1^{(k)}(\Phi^*) = \sum_{h=0}^{\mathcal{N}-1} \frac{\tilde{\beta}_h^{(k)}}{\sqrt{\Omega_h}} \Phi_h^* \ . \tag{25}$$

In the $\tilde{G} = 1/2$ case all the $\tilde{\beta}_h^{(0)}$ are sizable, reflecting the high degree of collectivity of the state, although the weight of the s-quasibosons living in single particle states with higher degeneracy, and hence more distant from the collective state, tends to be greater. For $\tilde{G} = 1/15$ the force is too weak to organise any collective motion.

Concerning the eigenstates of the trapped solutions when $\tilde{G}$ is large, the k=1 and 2 states approach the lower unperturbed levels, and so do their wave functions: in fact in the left panel one sees that the dominant component of the latter corresponds to $h = k - 1$. Instead the energies of the k=3 and 4 states occur close to the middle of two unperturbed energies: hence their wave functions display *two* dominant components. For small $\tilde{G}$ the energies of the trapped solutions remain close to the unperturbed energies, hence their wave function almost coincide with the unperturbed $h = k$ state.

3 The collective solution

We first consider the collective solution in the extreme situation where all the levels coalesce. Then eq. (22) reduces to

$$\frac{\Omega}{2\overline{e} - E} = \frac{1}{G} \tag{26}$$

(with $\Omega = \sum_\nu \Omega_\nu$ and $e_\nu = \overline{e}\ \forall \nu = 1, \ldots, L$), entailing

$$E = 2\overline{e} - \Omega G \ . \tag{27}$$

Thus in this limit only the collective state survives. Clearly (27) remains a good approximation when the degeneracies of the L levels are lifted only if their spread in energy is small with respect to ΩG. An accurate analytic solution when the distribution of the levels is arbitrary will be derived in the next subsection in both the large and small G limits.

3.1 The 'strong coupling' limit

For large G it is convenient to recast eq. (22) as

$$\sum_\nu \frac{\Omega_\nu}{2e_\nu - E} = -\frac{1}{E-2\bar{e}} \sum_\nu \frac{\Omega_\nu}{1 - 2\dfrac{e_\nu - \bar{e}}{E-2\bar{e}}} = \frac{1}{G} \ . \tag{28}$$

and expand in the parameter $2(e_\nu - \bar{e})/(E - 2\bar{e})$. Defining

$$\bar{e} = \frac{\sum_\nu \Omega_\nu e_\nu}{\Omega} \tag{29}$$

in leading order we get

$$E_0 = 2\bar{e} - \Omega G \ , \tag{30}$$

which coincides with the degenerate case value (27). Importantly, owing to the definition (29), the next-to-leading order correction vanishes.

To proceed further we rewrite (28) as

$$-\frac{\Omega}{E-2\bar{e}} \sum_{n=0}^{\infty} \frac{2^n M^{(n)}}{(E-2\bar{e})^n} = -\frac{\Omega}{E-2\bar{e}} \sum_{n=0}^{\infty} \left(\frac{G\Omega}{E-2\bar{e}} \right)^n m^{(n)} \alpha^n = \frac{1}{G} \ , \tag{31}$$

where the generalised moments of the distribution of single particle levels e_ν, namely

$$M^{(n)} = \sigma^n m^{(n)} = \frac{1}{\Omega} \sum_\nu \Omega_\nu (e_\nu - \bar{e})^n \ , \tag{32}$$

have been introduced together with the expansion parameter

$$\alpha = \frac{2\sigma}{G\Omega} \tag{33}$$

and the variance

$$\sigma = \sqrt{\frac{1}{\Omega} \sum_\nu \Omega_\nu (e_\nu - \bar{e})^2} \tag{34}$$

of the level distribution. The 'strong coupling' regime then corresponds to $\alpha \ll 1$. Note that the second moment is the square of the variance σ, whereas

the third, $M^{(3)} = \sigma^3\gamma$, and fourth, $M^{(4)} = (c+3)\sigma^4$, moments are related to the skewness γ and to the kurtosis c of the distribution, respectively.

In a perturbative scheme, setting $E^{(n)} = E^{(n-1)} + \delta$ and linearising in δ, we get for the collective energy

$$\frac{E - 2\bar{e}}{G\Omega} = -1 - \alpha^2 + \gamma\alpha^3 - (1+c)\alpha^4 + \mathcal{O}(\alpha^5) \ , \tag{35}$$

or, equivalently,

$$E \simeq -G\Omega + 2\bar{e} - \frac{4\sigma^2}{G\Omega} + \frac{8\gamma\sigma^3}{G^2\Omega^2} - \frac{16(1+c)\sigma^4}{G^3\Omega^3} \ , \tag{36}$$

an expression valid for $\alpha \ll 1$ and independent of the single particle energies distribution.

3.2 The 'weak coupling' limit

When $\alpha > 1$ the collectivity is very weak (see Fig. 2, right panel) and in (28) the term $\nu = 1$ dominates the sum. Thus by separating the latter we rewrite (28) in the form

$$\sum_{\nu=2}^{L} \frac{\Omega_\nu}{2(e_\nu - e_1) - (E - 2e_1)} + \frac{\Omega_1}{2e_1 - E} = \frac{1}{G} \ . \tag{37}$$

Now, for $G \simeq 0$, the quantity $2e_1 - E$ is of the order of G: hence the last term in the lhs of (37) dominates. Thus the leading contribution to the energy is

$$E_0 = 2e_1 - G\Omega_1 \ . \tag{38}$$

Factorising then $2(e_\nu - e_1)$ in the denominator of (37), expanding in powers of $(E - 2e_1)/2(e_\nu - e_1)$ and introducing the inverse generalised moments

$$M^{(-r)} = \frac{m^{(-r)}}{\sigma^r} = \frac{1}{\Omega - \Omega_1} \sum_{\nu=2}^{L} \frac{\Omega_\nu}{(e_\nu - e_1)^r} \tag{39}$$

we get

$$\frac{G(\Omega - \Omega_1)}{2\sigma} \left[m^{(-1)} + \frac{E - 2e_1}{2\sigma} m^{(-2)} + \left(\frac{E - 2e_1}{2\sigma} \right)^2 m^{(-3)} + \cdots \right]$$

$$-\frac{G\Omega_1}{E-2e_1}=1\ . \quad (40)$$

Proceeding then as in section 3.1, we next expand in powers of $\beta \equiv m^{(-1)}/\alpha'$, being $1/\alpha' = G(\Omega-\Omega_1)/2\sigma$. At the order β^3 we obtain

$$\begin{aligned}\frac{E-2e_1}{G\Omega_1} &\simeq -\left\{1+\beta+\beta^2\left[1-\frac{m^{(-2)}}{(m^{(-1)})^2}\frac{\Omega_1}{\Omega-\Omega_1}\right]\right. \quad (41)\\ &+ \left.\beta^3\left[1-3\frac{m^{(-2)}}{(m^{(-1)})^2}\frac{\Omega_1}{\Omega-\Omega_1}+\frac{m^{(-3)}}{(m^{(-1)})^3}\left(\frac{\Omega_1}{\Omega-\Omega_1}\right)^2\right]\right\}\ ,\end{aligned}$$

where α' does not coincide with $1/\alpha$ because the lowest unperturbed state has been separated out. Note that not only where the 'strong coupling' expansion fails the 'weak coupling' one holds valid, but also an overlap region appears to exist where both expansions yield quite accurate results, being at the same time $\alpha < 1$ and $\beta < 1$.

3.3 The Euler-McLaurin approximation

An interesting approach to the pairing problem is offered by the Euler-McLaurin formula [6]. It enables us to replace the sum with an integral, i.e.[1]

$$\sum_{\nu=a}^{b} f(\nu) = \frac{1}{2}f(a)+\frac{1}{2}f(b)+\int_a^b f(u)du + R\ . \quad (42)$$

The formula (42) holds valid if $f(\nu)$, ν to be viewed as a complex variable, is analytic in the strip $a \le \mathrm{Re}\nu \le b$ (a and b being integers). Neglecting the last term in the rhs, we shall illustrate the use of (42) in the case of the harmonic oscillator well, whose levels we label with an index $k = 0, 1, \cdots \mathcal{N}-1$. For this potential, from the well-known unperturbed energies

$$e_k \equiv \tilde{e}_k \hbar\omega_0 = (k+3/2)\hbar\omega_0 \quad (43)$$

and associated pair degeneracies

$$\Omega_k = (k+1)(k+2)/2\ , \quad (44)$$

[1]The function R was first fixed by Euler to be $\int_a^b (u-[u]-1/2)f'(u)du$. McLaurin provided more accurate expressions for it.

the total degeneracy Ω, the average energy $\bar{e}$ and the variance σ are found to be

$$\Omega = \frac{1}{6}\mathcal{N}(\mathcal{N}+1)(\mathcal{N}+2) \ , \tag{45}$$

$$\overline{e} = \frac{3}{4}(\mathcal{N}+1)\hbar\omega_0 \tag{46}$$

and

$$\sigma^2 = \frac{3}{80}(\mathcal{N}-1)(\mathcal{N}+3)(\hbar\omega_0)^2 \ , \tag{47}$$

respectively. The above entail

$$\alpha^{(h.o.)} = \frac{3\hbar\omega_0}{G}\sqrt{\frac{3}{5}}\frac{\sqrt{(\mathcal{N}-1)(\mathcal{N}+3)}}{\mathcal{N}(\mathcal{N}+1)(\mathcal{N}+2)} \ . \tag{48}$$

Incidentally, from (48) the coincidence of (36) at the order α^2 with the finding of ref. [2] follows.

Before exploiting (42) we recast (22) using the digamma functions and the dimensionless variables $\tilde{G} \equiv G/\hbar\omega_0$ and $\tilde{E} \equiv E/\hbar\omega_0$; we get

$$\begin{aligned} F^{\mathcal{N}}(\tilde{E}) &\equiv \sum_{N=0}^{\mathcal{N}-1} \frac{(N+1)(N+2)}{2N+3-\tilde{E}} \\ &= \frac{\mathcal{N}(2+\tilde{E}+\mathcal{N})}{4} + \frac{\tilde{E}^2-1}{8}\left[\psi\left(\mathcal{N}+\frac{3-\tilde{E}}{2}\right) - \psi\left(\frac{3-\tilde{E}}{2}\right)\right] \\ &= \frac{\mathcal{N}(2+\tilde{E}+\mathcal{N})}{4} \\ &+ \frac{\tilde{E}^2-1}{8}\left[\psi\left(\mathcal{N}+\frac{1-\tilde{E}}{2}\right) - \psi\left(\frac{3-\tilde{E}}{2}\right) + \frac{2}{1+2\mathcal{N}-\tilde{E}}\right] = \frac{2}{\tilde{G}} \ . \end{aligned} \tag{49}$$

In the 'strong coupling' limit the collective solution is strongly pushed down in energy, hence the use of the asymptotic formula

$$\psi(z) \sim \ln z - \frac{1}{2z} - \sum_{k=1}^{\infty} \frac{B_{2k}}{2kz^{2k}} \ , \tag{50}$$

the B_{2k} being the Bernoulli numbers, is appropriate. It is then remarkable that by inserting the ψ as given by the first two terms on the rhs of (50) into (49) one obtains the same expression provided by the Euler-McLaurin formula for the harmonic oscillator, namely

$$F^{\mathcal{N}}_{\mathrm{E-McL}}(\tilde{E}) = \frac{\mathcal{N}(2+\tilde{E}+\mathcal{N})}{4} + \frac{\tilde{E}^2-1}{8}\left[\frac{1}{3-\tilde{E}} + \frac{1}{2\mathcal{N}+1-\tilde{E}} + \ln\frac{2\mathcal{N}+1-\tilde{E}}{3-\tilde{E}}\right] . \tag{51}$$

In the tables 1 and 2 we refer to the eigenvalues obtained using (51) as ML. Furthermore, being the term z^{-3} absent in (50), to keep in the expansion (50) also the $k=1$ terms yields excellent results. We refer to this approximation as $ML2$.

3.4 Numerical results for the collective energy

In this subsection we present our predictions for the collective energy, essentially in the harmonic oscillator case, for $\tilde{G}$=0.1 and 0.2 (a realistic estimate for atomic nuclei with mass number $A > 100$). Our results, corresponding to eqs. (35), (41) and to the solution eq. (49) with $F^{\mathcal{N}}$ given by (51), are shown in tables 1, 2 and compared with the exact solutions for some values of $\mathcal{N}$.

$\mathcal{N}$	$\tilde{E}_{\mathrm{exact}}$	$\mathcal{O}(\alpha^2)$	$\mathcal{O}(\alpha^4)$	α	$\mathcal{O}(\beta)$	$\mathcal{O}(\beta^3)$	β	$\tilde{E}_{\mathrm{ML}}$	$\tilde{E}_{\mathrm{ML2}}$
2	2.883	–	–	2.17	2.885	2.883	0.15	2.927	2.822
3	2.860	–	–	1.34	2.87	2.860	0.3	2.909	2.800
4	2.820	3.925	1.479	0.89	2.853	2.825	0.47	2.877	2.763
6	2.529	3.695	2.930	0.46	2.814	2.681	0.86	2.590	2.500
8	0.1361	0.5375	0.2161	0.28	–	–	1.35	0.1338	0.1362
10	-6.477	-6.298	-6.461	0.19	–	–	1.95	-6.459	-6.477
12	-17.68	-17.58	-17.68	0.14	–	–	2.63	-17.64	-17.68

Table 1: Comparison between the exact and the approximate collective energy for the harmonic oscillator case, for various values of $\mathcal{N}$ and $\tilde{G} = 0.1$. The energies are in units of $\hbar\omega_0$. Columns 3 and 4: strong coupling; columns 6 and 7: weak coupling; columns 9 and 10: Euler-McLaurin approximations.

$\mathcal{N}$	$\tilde{E}_{\rm exact}$	$\mathcal{O}(\alpha^2)$	$\mathcal{O}(\alpha^4)$	α	$\mathcal{O}(\beta)$	$\mathcal{O}(\beta^3)$	β	$\tilde{E}_{\rm ML}$	$\tilde{E}_{\rm ML2}$
2	2.728	–	–	1.1	2.74	2.727	0.3	2.796	2.677
3	2.583	3.1	2.185	0.67	2.68	2.589	0.6	2.653	2.547
4	2.182	2.713	2.243	0.44	2.613	2.318	0.93	2.224	2.171
6	-1.480	-1.303	-1.461	0.23	–	–	1.73	-1.478	-1.480
8	-11.06	-10.98	-11.05	0.14	–	–	2.71	-11.01	-11.06
10	-27.94	-27.90	-27.94	0.10	–	–	3.88	-27.85	-27.94
12	-53.66	-53.64	-53.66	0.07	–	–	5.25	-53.53	-53.66

Table 2: Same as table 1 for $\tilde{G} = 0.2$.

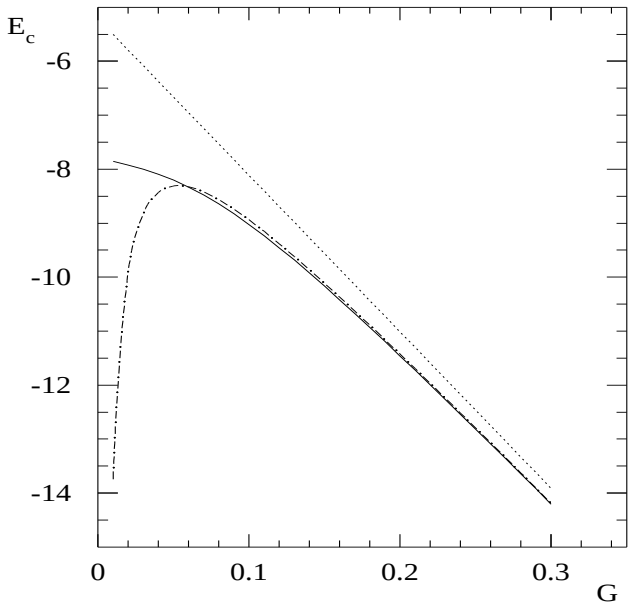

Figure 3: The collective energy of ^{210}Pb as a function of the pairing strength G (in MeV). Solid line: exact numerical solution; dotted: degenerate solution (order α^0); dot-dashed: the approximation (35) at the order α^2.

The approximate energies (35) are in good agreement with the exact ones for $\tilde{G} \geq 0.2$. Instead for smaller $\tilde{G}$ and $4 \leq \mathcal{N} \leq 8$ the collective energy in the 'weak coupling' limit, namely eq. (41), is in better touch with the exact values. The existence of a region where both the 'strong' and the 'weak' approximations hold valid, is apparent. We also quote in the tables 1, 2 the results obtained with the McLaurin approximation in first and second order, as previously discussed.

To address a situation of physical interest, we consider the case of ^{210}Pb, where one pair of neutrons lives in the $N = 6$ shell, set up with the s.p. levels $d_{3/2}$, $g_{7/2}$, $s_{1/2}$, $d_{5/2}$, $j_{15/2}$, $i_{11/2}$ and $g_{9/2}$ of energies –1.5, –1.6, –2.0, –2.3, –2.4, –3.1 and –3.9 MeV, respectively. The total degeneracy Ω, the average energy value $\bar{e}$, see (29), and the variance σ then turn out to be 29, –2.61 and 0.77 MeV, respectively. Since for lead $G \simeq 0.1$ MeV we obtain $\alpha = 0.53$ and $\beta = 0.89$. Hence we are in the 'strong coupling' limit.

In Fig. 3 we compare the collective energy (35) for ^{210}Pb, at order α^0 and at order α^2, with the exact numerical solution as functions of G: we see that, in the physical range of G, an excellent accord with the exact result is obtained when the term α^2 is included.

4 Trapped solutions

4.1 The general case

The evaluation of the trapped eigenvalues can be easily performed numerically. This approach however hides the interesting pattern the trapped solutions display, already suggested in [2] where they were associated with a quantum number and a parabolic behaviour in the latter was shown to occur for a harmonic oscillator well.

To shed light on this aspect of the pairing problem we first observe that, irrespectively of the strength of the interaction, $2e_{\nu-1} < E^{(\nu)} < 2e_\nu$, $E^{(\nu)}$ being the energies of the trapped solutions ($\nu = 2, \ldots L$).

Next we define a new variable $z^{(\nu)}$ according to

$$E^{(\nu)} = 2e_{\nu-1} + 2z^{(\nu)}(e_\nu - e_{\nu-1}) \tag{52}$$

(clearly $z^{(\nu)} \in (0, 1)$) and select from the secular equation the terms associ-

ated with the poles in $2e_{\nu-1}$ and $2e_\nu$, thus getting

$$\frac{\Omega_{\nu-1}}{z^{(\nu)}} + \frac{\Omega_\nu}{z^{(\nu)}-1} = \varphi_\nu(z^{(\nu)}) \tag{53}$$

with

$$\begin{aligned}\varphi_\nu(z^{(\nu)}) &= \sum_{\substack{\mu=1\\ \mu\neq\nu,\nu-1}} \frac{\Omega_\mu}{\dfrac{e_\mu - e_{\nu-1}}{e_\nu - e_{\nu-1}} - z^{(\nu)}} - \frac{2(e_\nu - e_{\nu-1})}{G} \\ &= \sum_{\substack{\mu=1\\ \mu\neq\nu,\nu-1}} \zeta(\mu, z) - \frac{2(e_\nu - e_{\nu-1})}{G} \ . \end{aligned} \tag{54}$$

We have thus isolated in the lhs of (53) the poles trapping the solution $z^{(\nu)}$ in the interval $(0,1)$. Now we approximate the rhs. To this purpose we expand in powers of $z^{(\nu)}$ ($\mu \neq \nu, \nu-1$):

$$\zeta(\mu, z) = \begin{cases} \displaystyle\sum_{n=0}^{\infty} \frac{\Omega_\mu z^n}{\left(\dfrac{e_\mu - e_{\nu-1}}{e_\nu - e_{\nu-1}}\right)^{n+1}} & \text{if } \ \mu > \nu \\ \\ \displaystyle\sum_{n=0}^{\infty} \frac{\Omega_\mu (1-z)^n}{\left(\dfrac{e_\nu - e_\mu}{e_\nu - e_{\nu-1}}\right)^{n+1}} & \text{if } \ \mu < \nu - 1 \ . \end{cases} \tag{55}$$

Of course (55), truncated at the order m, provides a polynomial approximation for the function φ.

Next we let the discrete variable ν become continuous by means of the Euler-McLaurin formula (42). We thus obtain for φ the expression

$$\begin{aligned}\varphi^{\mathrm{E-McL}}(\nu, z) = \frac{1}{2}\zeta(1,z) + \frac{1}{2}\zeta(\nu-2,z) + \int_1^{\nu-2} \zeta(\mu,z)d\mu \\ + \frac{1}{2}\zeta(\nu+1,z) + \frac{1}{2}\zeta(L,z) + \int_{\nu+1}^{L} \zeta(\mu,z)d\mu \\ - \frac{2[e(\nu) - e(\nu-1)]}{G} \ , \end{aligned} \tag{56}$$

which is analytic in the variable ν, if e_ν and Ω_ν have been analytically extended.

Approximate expressions for $z^{(\nu)}$ then follow from the continuous version of (53), namely

$$\frac{\Omega(\nu-1)}{z(\nu)}+\frac{\Omega(\nu)}{z(\nu)-1}=\varphi^{\mathrm{E-McL}}(\nu,z)\ , \tag{57}$$

which implicitly defines z as a function of the complex variable ν. The simplest approximation corresponds to replace the rhs with $\varphi^{\mathrm{E-McL}}(\nu,0)$. One gets

$$\begin{aligned} z_0(\nu) = & \frac{\varphi^{\mathrm{E-McL}}(\nu,0)+\Omega(\nu-1)+\Omega(\nu)}{2\varphi^{\mathrm{E-McL}}(\nu,0)} \\ & - \frac{\sqrt{[\varphi^{\mathrm{E-McL}}(\nu,0)+\Omega(\nu-1)+\Omega(\nu)]^2-4\Omega(\nu-1)\varphi^{\mathrm{E-McL}}(\nu,0)}}{2\varphi^{\mathrm{E-McL}}(\nu,0)}\ , \end{aligned} \tag{58}$$

which can be further simplified via a parabolic expansion around, e.g., the middle point $\nu=L/2$, namely

$$z_0(\nu)\simeq z_0(L/2)+\left(\nu-\frac{L}{2}\right)z_0{}'(L/2)+\frac{1}{2}\left(\nu-\frac{L}{2}\right)^2 z_0{}''(L/2)\ . \tag{59}$$

To further proceed a specific model for $\Omega(\nu)$ and $e(\nu)$ should be chosen, which we shall do in the next subsection. Here we display the numerical results for the case of ^{210}Pb already discussed in subsec. 3.4. In tab. 3 we display both $z_0(\nu)$ as given by (58) and $z_1(\nu)$ (namely the $z(\nu)$ obtained by truncating (55) at first order and then by solving the corresponding equation by successive linearisations) together with the exact numerical solutions. The corresponding energies, see (52), are also reported.

4.2 The harmonic oscillator case

In this subsection the functions $\Omega(\nu)$ and $e(\nu)$ are those of the harmonic oscillator. As in sec. 3.3, we label the solutions with the index k, $1\le k\le \mathcal{N}-1$ (the value $k=0$ corresponds to the collective solution).

Using the dimensionless variables $\tilde{E}$, $\tilde{G}$ and $\tilde{z}=z/\hbar\omega_0$ we rewrite (53) in the Euler-McLaurin approximation (56) obtaining

$$\frac{\Omega(k-1)}{\tilde{z}(k)}+\frac{\Omega(k)}{\tilde{z}(k)-1}=\varphi^{\mathrm{E-McL}}(k,\tilde{z}(k)) \tag{60}$$

ν	$z^{\rm exact}$	z_0	z_1	$E^{\rm exact}$	E_0	E_1
2	0.560	0.621	0.577	-6.903	-6.807	-6.876
3	0.555	0.605	0.577	-5.423	-5.353	-5.392
4	0.760	0.762	0.760	-4.648	-4.648	-4.648
5	0.929	0.934	0.931	-4.043	-4.040	-4.041
6	0.730	0.749	0.748	-3.416	-3.401	-3.402
7	0.783	0.782	0.783	-3.043	-3.043	-3.043

Table 3: Exact and approximate energies for the trapped levels in the case of ^{210}Pb. The E's are in MeV, the z's are pure numbers.

with

$$\begin{aligned}\varphi^{\rm E-McL}(k,\tilde{z}) = &-\frac{2}{\tilde{G}} - \frac{3}{4}(4k+2\tilde{z}+3) + \frac{1}{4}(\mathcal{N}-1)(\mathcal{N}+2k+2\tilde{z}+3) \\ &+ \frac{k(1-k)}{4(\tilde{z}+1)} - \frac{(k+2)(k+3)}{4(\tilde{z}-2)} \\ &- \frac{1}{2(k+\tilde{z}-1)} - \frac{\mathcal{N}(\mathcal{N}+1)}{4(k+\tilde{z}-\mathcal{N})} \\ &+ \frac{1}{2}(k+\tilde{z})(k+\tilde{z}+1)\log\left|\frac{(\tilde{z}+1)(k+\tilde{z}-\mathcal{N})}{(\tilde{z}-2)(k+\tilde{z}-1)}\right| \ .\end{aligned} \tag{61}$$

The Euler-McLaurin approximation is not only valid quantitatively, but also provides the key for studying analytically limiting cases (like $\mathcal{N} \to \infty$), which are helpful in shedding light on the properties of the trapped eigenvalues. Indeed consider eq. (60): on the lhs it displays the usual two poles in the complex plane of $\tilde{z}$, at 0 and 1, respectively, whereas the rhs has poles at $\tilde{z}$=–1 and 2. Equivalently, in the variable $\tilde{E}^{(k)}$, the poles in the range from $\tilde{E}^{(k-2)}$ to $\tilde{E}^{(k+1)}$ are explicitly kept, while the others are simulated by two cuts. The graphical solution is shown in Fig. 4 where the quantity

$$-\frac{\Omega(k-1)}{\tilde{z}(k)} - \frac{\Omega(k)}{\tilde{z}(k)-1} + \varphi^{\rm E-McL}(k,\tilde{z}(k)) + \frac{2}{\tilde{G}} \tag{62}$$

(as a function of $\tilde{E}$) is plotted. The eigenvalues correspond to the intersections with the straight line $2/\tilde{G}$. Four solutions are found: the collective one is of no interest here, the other three correspond to the indices $k-1$, k and

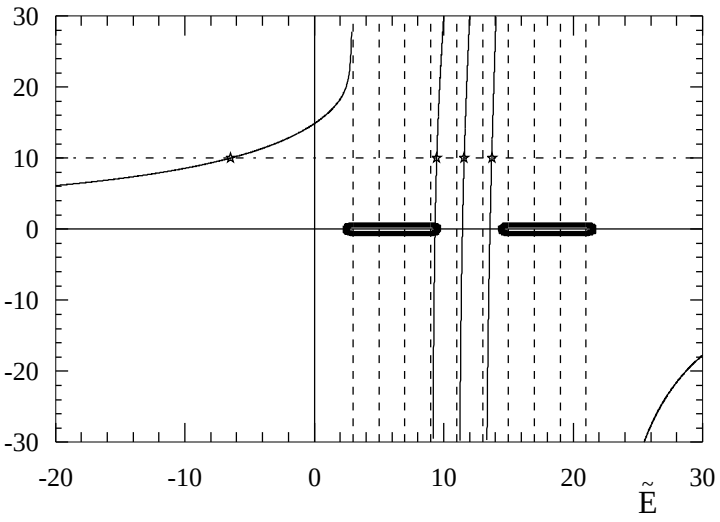

Figure 4: Graphical solution of the secular equation in the Euler-McLaurin approximation. Only the part of the curves outside the cuts (displayed as a black area) is drawn.

$k+1$. We shall only keep the middle solution, the most accurate, as it lies far from both the left and the right cut.

The results of the Euler-McLaurin approximation for the trapped energies are shown in Figs. 6 and 7, as a solid line.

We now explore on the basis of (60) the $\mathcal{N} \to \infty$ limit. For this purpose we introduce the variable

$$\lambda = \frac{k}{\mathcal{N}} \ . \tag{63}$$

Clearly, when $\mathcal{N}$ is large, $\lambda \in (0,1)$.

Also we express the coupling constant $\tilde{G}$ in terms of α according to (48). Then eq. (60) becomes

$$\begin{aligned} &\frac{1}{\tilde{z}} + \frac{1}{\tilde{z}-1} + \frac{1}{2(\tilde{z}+1)} + \frac{1}{2(\tilde{z}-2)} - \log\left|\frac{\tilde{z}+1}{\tilde{z}-2}\right| \\ &= \frac{1}{\lambda} + \log\frac{1-\lambda}{\lambda} + \frac{1-\frac{8}{3}\sqrt{\frac{5}{3}}\alpha}{2\lambda^2} \ , \end{aligned} \tag{64}$$

the $\tilde{z}$-dependence appearing only in the lhs, referred to as $\phi(\tilde{z})$, and the λ dependence only in the rhs, referred to as $\xi_\infty(\lambda)$.

Eq. (64) is easily solved numerically and the results are displayed in Fig. 5 for different values of α.

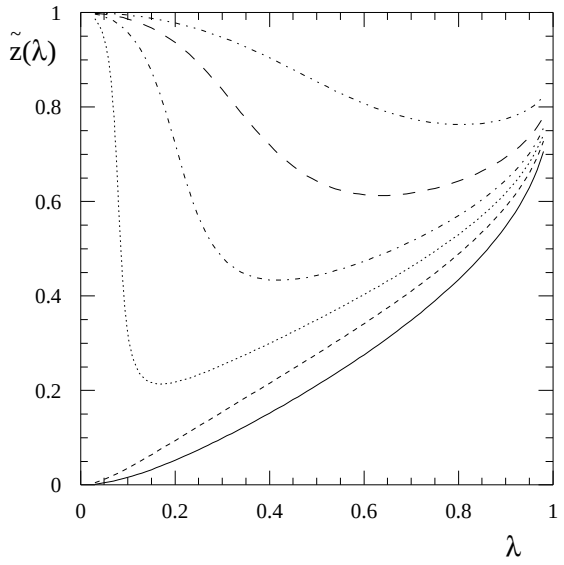

Figure 5: Solution of the eigenvalue equation in the limit $\mathcal{N} \to \infty$ in the Euler-McLaurin approximation for different values of α. Solid line: $\alpha = 0$, dashed line: $\alpha = 0.2$, dotted line: $\alpha = 0.35$, dash-dotted line: $\alpha = 0.5$, long-dashed line: $\alpha = 0.8$, dot-dot-dashed line: $\alpha = 1.5$. The exact results are not displayed as they almost coincide with the ones in the figure.

Of significance is the $\alpha \to 0$ case, which still carries the fingerprints of the harmonic oscillator and the $\alpha \to \infty$ one, which corresponds to the straight line $\tilde{z} = 1$. It is of great interest to follow the behaviour with α of the curves. The sum of the eigenvalues, or, better, of the $\tilde{z}(\lambda)$, offers a guidance to globally follow this evolution. Actually this "sum rule" for the

trapped solutions can be *exactly* computed in the two limiting cases $\alpha = 0$ and $\alpha = \infty$. Indeed from the Viète equations one has

$$\Sigma(\alpha = 0) \equiv \frac{1}{\mathcal{N}-1} \sum_{k=1}^{\mathcal{N}-1} \tilde{z}(k) = \frac{1}{4} \tag{65}$$

and $\Sigma(\alpha = \infty) = 1$, respectively: these values set the limits for the area under the curves of Fig. 5.

On the other hand the behaviour of the curves themselves is ruled both by the function $\xi_\infty(\lambda)$, which goes to $-\infty$ when $\lambda \to 1$, whereas for $\lambda \to 0$

$$\xi_\infty(\lambda) \underset{\lambda \to 0}{\longrightarrow} \begin{cases} +\infty & \text{for } \alpha < \alpha_{\rm cr} \\ -\infty & \text{for } \alpha > \alpha_{\rm cr} \end{cases} \qquad \text{with} \quad \alpha_{\rm cr} = \frac{3}{8}\sqrt{\frac{3}{5}} \simeq 0.29 \ , \tag{66}$$

and by the monotonic decrease of $\phi(\tilde{z})$ in the interval $(0, 1)$, which varies within the limits

$$\lim_{\tilde{z} \to 0} \phi(\tilde{z}) = +\infty \qquad\qquad \lim_{\tilde{z} \to 1} \phi(\tilde{z}) = -\infty \ . \tag{67}$$

Thus, when $\lambda \to 1$,

$$\tilde{z}(\lambda) \to 1 + \frac{1}{4 \log(1-\lambda)} \tag{68}$$

no longer depends upon α and slowly approaches 1.

For $\lambda \to 0$ two cases occur: if $\alpha < \alpha_{\rm cr}$ then $\tilde{z}(\lambda) \to 0$, if $\alpha > \alpha_{\rm cr}$ instead $\tilde{z}(\lambda) \to 1$. Thus a transition occurs at $\alpha_{\rm cr}$: indeed the exact eigenvalue arises by perturbing the $(k-1)$-th free one when $\alpha < \alpha_{\rm cr}$ (strong coupling regime), according to (53), and by perturbing the k-th one when $\alpha > \alpha_{\rm cr}$ (weak coupling regime) according to

$$E^{(\nu)} = 2e_\nu - 2z^{(\nu)}(e_\nu - e_{\nu-1}) \ . \tag{69}$$

This is strikingly illustrated in Fig. 5 that shows that the almost parabolic behaviour of $\tilde{z}(\lambda)$ for small α is strongly distorted for $\alpha \simeq \alpha_{\rm cr}$ for small λ. For larger α a smoother behaviour is recovered. In particular in Fig. 5 a marked minimum is seen to develop for α above, but close to, the critical value. When $\mathcal{N}$ is finite, for $\lambda < 1/\mathcal{N}$, there are no eigenvalues, since $\tilde{z}$ lives on a discrete set of points: hence $\alpha_{\rm cr}$ is ill-defined.

A deeper insight of the above findings is offered by the following comments:

1. the pairing interaction is of finite range, therefore a pair trapped by highly excited harmonic oscillator states has the two partners extremely de-localised, hence unaffected by the interaction. This explains why all the curves in Fig. 5 coalesce to 1 when $\lambda \to 1$, no matter what the value of α is. On the other hand all the curves (up to a critical value of α) converge to $\tilde{z}(0) = 0$, reflecting the pressure exercised by the infinite number of the high-lying, large degeneracy, levels on the low-lying, low-degeneracy, ones.

2. The eigenvalues obey a "sum rule", whose value grows with α from 1/4 to 1 , hence they must grow as well: since the action of the pairing force is gauged by the product $G\Omega_k$, at some critical value of α (hence for G sufficiently small) the system prefers to fulfil the sum rule by lifting the lowest eigenvalues (corresponding to the lowest degeneracies) to the unperturbed values. Indeed (see next section) when the degeneracy of the harmonic oscillator levels is artificially made to decrease, then no transition occurs.

In concluding this section we turn to the problem of finding analytical expressions for the trapped eigenvalues. In this connection we first notice that, remarkably, the large $\mathcal{N}$ limit is still a good approximation to the exact solutions even for $\mathcal{N} = 5$, as shown in Fig. 6. While in this limit the complexity of the lhs of eq. (64) is still such to render difficult the finding of simple analytical approximations, yet its structure is dominated by the poles in 0 and 1 that trap the solution.

It is thus reasonable to approximate $\phi(\tilde{z})$ with

$$\phi^{\rm appr}(\tilde{z}) = \frac{11}{9}\left(\frac{1}{\tilde{z}} + \frac{1}{\tilde{z}-1}\right) , \tag{70}$$

which retains the pole structure and reproduces $\phi(\tilde{z})$ together with its two first derivatives at $\tilde{z} = 1/2$. Hence, from the equation (64), $\phi^{\rm appr}(\tilde{z}) = \xi_\infty(\lambda)$, it follows

$$\tilde{z}^{\rm appr}(\lambda) = \frac{1}{2} + \frac{11}{9\xi_\infty} - \frac{\sqrt{484 + 81\xi_\infty^2}}{18\xi_\infty} , \tag{71}$$

displayed as a dotted line in Figs. 6 and 7.

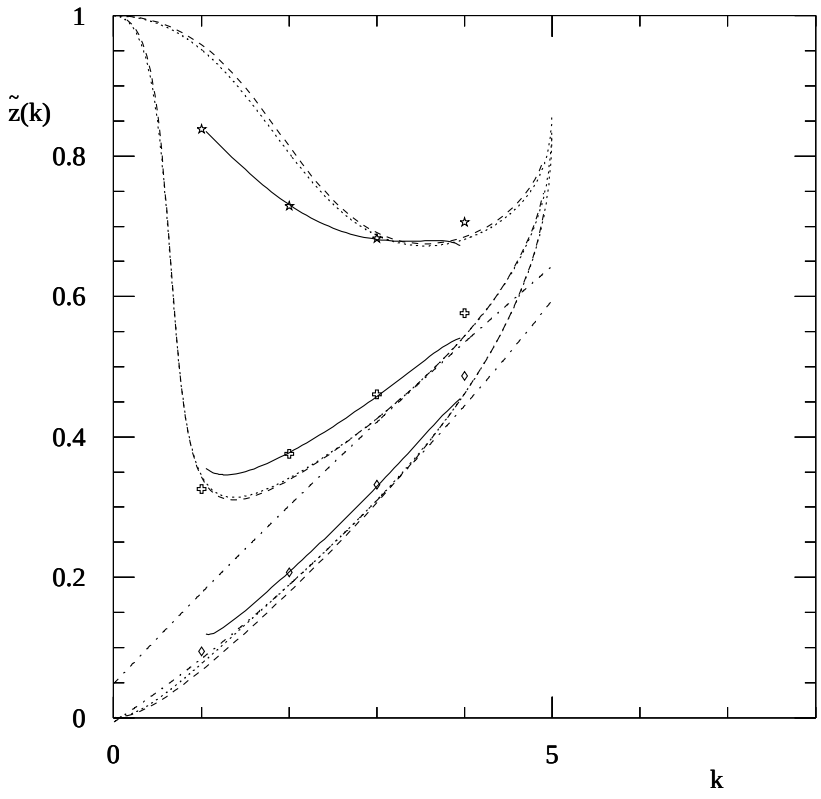

Figure 6: Exact and approximate values for the trapped solutions in the $\mathcal{N} = 5$ case at different values of α: diamonds: $\alpha = 0.1$, crosses: $\alpha = 0.4$, stars: $\alpha = 1$. Solid lines: Euler-McLaurin approximation, dashed lines: the same but in the limit $\mathcal{N} \to \infty$, dotted lines: approx. eq. (71), dash- dotted lines: parabolic approximation.

By expanding in λ (say around 1/2) and in α up to the second order a parabolic expression for $\tilde{z}$ as a function of λ is obtained, also shown in Figs. 6 and 7.

In these figures the Euler-McLaurin approximation in the case $\mathcal{N} \to \infty$ is

seen to be remarkably stable and in good accord with the exact eigenvalues when $\mathcal{N}$ is reduced to finite values for $\alpha < \alpha_{cr}$ (but not for $\alpha > \alpha_{cr}$). Furthermore the predictions of the simple expression eq. (71) almost superimpose to the Euler-McLaurin ones.

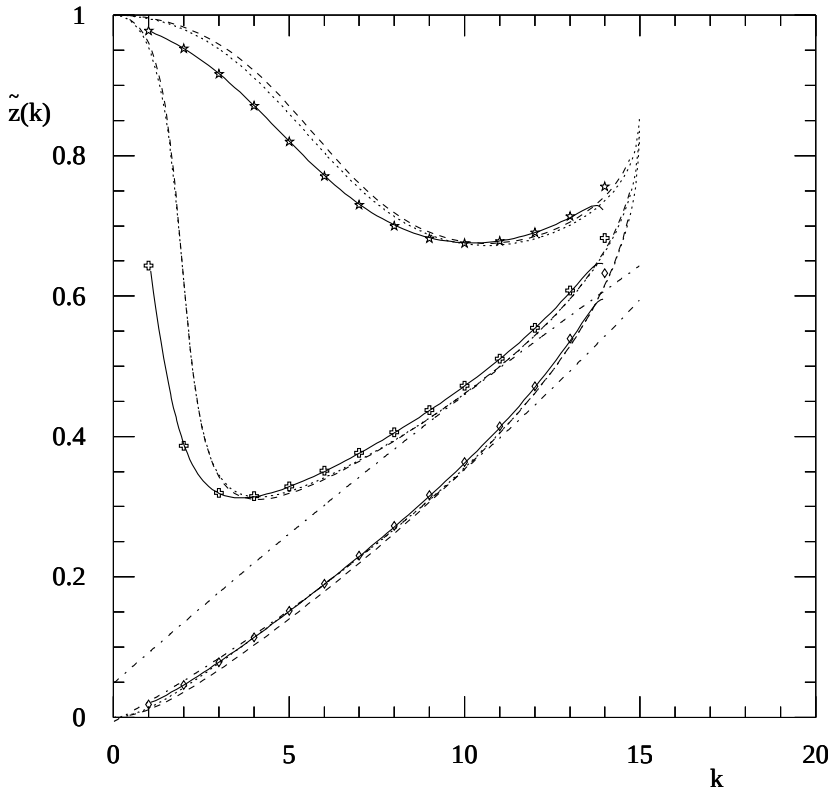

Figure 7: Same as in Fig. 6 but with $\mathcal{N} = 15$

4.3 Variations on the harmonic oscillator

In this subsection we explore whether the transition previously discussed occurs only in the case of the harmonic oscillator or is more general. Accordingly, we take $\mathcal{N}$ large and leave unchanged the regular arrangement of the harmonic oscillator eigenvalues, but vary, admittedly artificially, their degeneracy according to the prescriptions

$$\Omega_k^{(a)} = (k+1)^\gamma \simeq \mathcal{N}^\gamma \lambda^\gamma \tag{72}$$

$$\Omega_k^{(b)} = (\mathcal{N}-k)^\gamma \simeq \mathcal{N}^\gamma (1-\lambda)^\gamma \tag{73}$$

with $\gamma \geq 0$. From the above

$$\alpha^{(a)} = \alpha^{(b)} = \sqrt{\frac{(\gamma+1)^3}{(\gamma+3)}} \frac{2}{(\gamma+2)\tilde{G}\mathcal{N}^\gamma} \ . \tag{74}$$

Note that for γ=2 (74) yields $\alpha^{(a)}\big|_{\gamma=2} = \alpha^{(h.o.)}/2$ in the large $\mathcal{N}$ limit.

Now from eq. (56) one gets for the function $\varphi^{E-McL}(k,\tilde{z})$ in the $\mathcal{N}\to\infty$ limit and in the case (a)

$$\varphi^{E-McL}(k,\tilde{z}) \xrightarrow[\mathcal{N}\to\infty]{} -\frac{\lambda^\gamma \mathcal{N}^\gamma}{2}\left(\frac{1}{\tilde{z}+1}+\frac{1}{\tilde{z}-2}\right) - \mathcal{N}^\gamma \sqrt{\frac{3+\gamma}{(1+\gamma)^3}}(2+\gamma)\alpha^{(a)} + \mathcal{N}^\gamma \left\{ \rho(\lambda,\gamma) + \lambda^\gamma \log\left|\frac{(1+\tilde{z})(1-\lambda)}{(2-\tilde{z})\lambda}\right| \right\} \ , \tag{75}$$

(a similar expression holds for case (b)), where

$$\rho(\lambda,\gamma) = \int_0^1 \frac{x^\gamma - \lambda^\gamma}{x-\lambda} \tag{76}$$

is an *analytic* (hence well behaved) function of λ and goes to $1/\gamma$ when $\lambda \to 0$. Accordingly the secular equation can be recast in the form

$$\phi(\tilde{z}) = \log\left|\frac{1-\lambda}{\lambda}\right| + \frac{1}{\lambda^\gamma}\left[\rho(\lambda,\gamma) - \sqrt{\frac{\gamma+3}{(\gamma+1)^3}}(\gamma+2)\alpha^{(a)}\right] \tag{77}$$

in case (a) and

$$\phi(\tilde{z}) \;=\; \log\left|\frac{1-\lambda}{\lambda}\right| - \frac{1}{(1-\lambda)^{\gamma}}\left[\rho(1-\lambda,\gamma) + \sqrt{\frac{\gamma+3}{(\gamma+1)^3}}(\gamma+2)\alpha^{(b)}\right] \;, \tag{78}$$

in case (b), the lhs exactly coinciding with the one of eq. (64).

In the limits $\lambda \to 0$ (case (a)) and $\lambda \to 1$ (case (b)), the leading terms of (77) and (78) are

$$\frac{1}{\lambda^{\gamma}}\left[\frac{1}{\gamma} - \sqrt{\frac{\gamma+3}{(\gamma+1)^3}}(\gamma+2)\alpha^{(a)}\right] \tag{79}$$

and

$$-\frac{1}{(1-\lambda)^{\gamma}}\left[\frac{1}{\gamma} + \sqrt{\frac{\gamma+3}{(\gamma+1)^3}}(\gamma+2)\alpha^{(b)}\right] \tag{80}$$

respectively. Remarkably $\tilde{z}(\lambda)$ in the $\lambda \to 0$ limit goes to 0 or 1, according to the sign of (79) (case a), which is set by α. The critical value is

$$\alpha_{\rm cr}^{(a)} = \sqrt{\frac{(\gamma+1)^3}{\gamma+3}}\frac{1}{\gamma(\gamma+2)} \tag{81}$$

clearly behaving as $1/\gamma$ when $\gamma \to 0$. On the contrary, in the case (b) in the $\lambda \to 1$ limit $\tilde{z}(\lambda)$ always tends to 1, since (80) never changes sign.

Thus a transition occurs only if the degeneracy is growing with k and the 'strong coupling' domain becomes wider ($\alpha_{\rm cr}$ increases) as γ approaches zero: here the transition disappears. If the degeneracy decreases with k (case b), no transition exists.

The eigenvalues corresponding to the degeneracies (a) and (b) for $\alpha = 0$ are displayed in Fig. 8.

5 Conclusions

In this paper we have once more addressed the pairing problem with the scopes of finding approximate, but analytic, solutions for the eigenvalues and eigenvectors and of disclosing a surprising pattern displayed by the former.

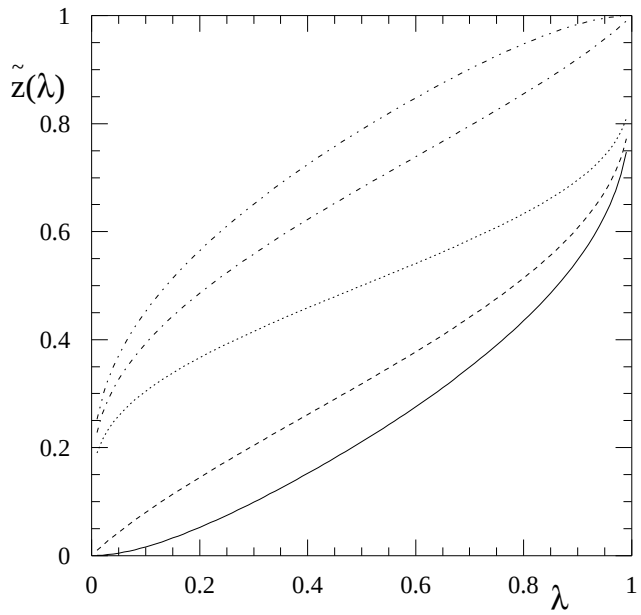

Figure 8: The functions $\tilde{z}(\lambda)$ for different degeneracies and $\alpha = 0$. Solid line: case a), $\gamma = 2$; dashed line: case a), $\gamma = 1$; dotted line: case a) and b) $\gamma = 0$; dash-dotted line: case b), $\gamma = 1$, dash-dotted-dotted line: case b), $\gamma = 2$.

To pave the way to the general problem with any number of pairs and levels we have addressed the simplified situation with only one pair living in a set of $\mathcal{N}$ single particle levels of a potential well.

For the collective mode we have found, in the strong and weak coupling regimes, expansions relating its energy not only to the strength of the pairing interaction, but as well to the parameters characterising the distribution of the single particle levels. Thus our analysis shows that different potential wells could lead to the same energy for the mode, which is accurately fixed by only a few parameters of the levels distribution and not by the precise energy of each of them. In particular the variance of the levels distribution appears crucial for the development of a collective mode.

Concerning the energies of the trapped solutions (when these are known,

so are the related eigenfunctions) our search for a simple formula for their description has in part been prompted by the recent finding [7] concerning the integrability of the pairing Hamiltonian, both at the quantum and at the classical level. Indeed it is reasonable to expect the existence of relatively simple analytic formulas for the eigenvalues of a Hamiltonian if the corresponding classical motion is not chaotic.

For this scope the Euler-McLaurin approximation, conveniently exploited, has been invaluable. We started from the extreme case of an infinite number of single particle levels of an harmonic oscillator and classified the trapped solutions in terms of a quantum number λ, varying between 0 and 1. For sufficiently large values of the pairing strength G the displacements of the trapped eigenvalues from the unperturbed solutions always start from 0 and monotonically grow to 1, reached when λ=1. The first of these findings relates to the "pressure" exercised by the high-lying eigenvalues (associated with very large degeneracy) on the low-lying ones, where the degeneracy is low. The second one instead relates to the delocalisation of the partners of the pair in very high-lying harmonic oscillator levels. Remember indeed that the pairing interaction is meant to simulate the short-range part of the nucleon-nucleon force: hence it is incapable of correlating two fermions lying far away from each other, provided no quasi-bound is generated by the interaction, as is the case for the trapped states.

In this connection it is worth reminding that the classical limit is achieved by letting the degeneracy of the single particle levels become very large [8]. Thus the coincidence of all the eigenvalues, for any G, in λ=1 also reflects the evolution from quantum to classical mechanics of our system.

Another aspect of significance of our work concerns the transition of the behaviour of the eigenvalues from one regime to another. Indeed we proved that a critical strength of the pairing force exists such that for weaker interactions the behaviour of the trapped eigenvalues versus λ ceases to be monotonic. Actually for all $G < G_{crit}$ the displacements of the eigenvalues from the unperturbed energies start from 1 rather than from 0. This occurrence might be understood on the basis of the sum rule the trapped solutions should fulfil and of the nature of the pairing force. In fact at some point the system prefers to obey the sum rule by lifting the lower eigenvalues (associated with low degeneracies) to values close to 1 (where the levels are associated with very large degeneracies).

Finally, from our analysis it emerges that the eigenvalues obtained in the $\mathcal{N} \to \infty$ are very robust with respect to variations of $\mathcal{N}$, when G is

large: indeed they keep their validity even for values of $\mathcal{N}$ as small as 5. Moreover, for $G > G_{crit}$, we have found that the trapped eigenvalues indeed lend themselves to simple analytical expressions, even to a parabolic one, as hinted in ref. [2].

We are presently investigating the statistical fluctuations of the trapped eigenvalues, which should reflect the integrability or, equivalently, the absence of chaotic motion associated to the pairing Hamiltonian.

References

[1] R. W. Richardson and N. Sherman, *Nucl. Phys.*, 52:221, 1964; R. W. Richardson, *Phys. Rev.*, 141:949, 1966.

[2] M. B. Barbaro, L. Fortunato, A. Molinari and M. R. Quaglia, *Phys. Rev.*, C64:011302, 2001.

[3] M. B. Barbaro, A. Molinari and F. Palumbo, *Nucl Phys.*, B 487:492, 1997.

[4] M. B. Barbaro, A. Molinari, F. Palumbo and M. R. Quaglia, *Phys. Lett.*, B 476:477, 2000.

[5] D. J. Rowe, *Nuclear Collective Motion*, Methuen and Co. LTD, London, 1970.

[6] G. Sansone and J. Gerretsen, *Lectures on the theory of functions of a complex variable*, P. Noordhoff, 1960.

[7] M. C. Cambiaggio, A. M. F. Rivas and M. Saraceno, *Nucl. Phys.*, A624:157, 1997.

[8] J. M. Román, G. Sierra and J. Dukelsky, cond-mat/0202070.